

# Transmembrane Topology and Oligomeric Structure of the High-affinity Choline Transporter\*

Received for publication, July 26, 2012, and in revised form, October 10, 2012. Published, JBC Papers in Press, November 6, 2012, DOI 10.1074/jbc.M112.405027

Takashi Okuda<sup>†S1</sup>, Chieko Osawa<sup>S</sup>, Haruhiko Yamada<sup>S</sup>, Kengo Hayashi<sup>S</sup>, Shizue Nishikawa<sup>S</sup>, Tomoko Ushio<sup>S</sup>, Yuji Kubo<sup>S</sup>, Motoyasu Satou<sup>S</sup>, Haruo Ogawa<sup>¶</sup>, and Tatsuya Haga<sup>S</sup>

From the <sup>†</sup>Department of Pharmacology, Faculty of Pharmacy, Keio University, 1-5-30 Shibakoen, Minato-ku, Tokyo 105-8512, the

<sup>S</sup>Department of Life Science, Faculty of Science, Gakushuin University, 1-5-1 Mejiro, Toshima-ku, Tokyo 171-8588, and the

<sup>¶</sup>Institute of Molecular and Cellular Biosciences, University of Tokyo, 1-1-1 Yayoi, Bunkyo-ku, Tokyo 113-0032, Japan

**Background:** The structure-function relationship of the high-affinity choline transporter CHT1 is largely unknown.

**Results:** Cysteine-scanning analysis and cross-linking/co-immunoprecipitation were used to determine the structural properties of CHT1.

**Conclusion:** CHT1 is a 13-transmembrane domain protein and forms a homo-oligomer on cell surface.

**Significance:** This might be the first molecular evidence of homo-oligomerization in the Na<sup>+</sup>/glucose cotransporter family (SLC5).

The high-affinity choline transporter CHT1 mediates choline uptake essential for acetylcholine synthesis in cholinergic nerve terminals. CHT1 belongs to the Na<sup>+</sup>/glucose cotransporter family (SLC5), which is postulated to have a common 13-transmembrane domain core; however, no direct experimental evidence for CHT1 transmembrane topology has yet been reported. We examined the transmembrane topology of human CHT1 using cysteine-scanning analysis. Single cysteine residues were introduced into the putative extra- and intracellular loops and probed for external accessibility for labeling with a membrane-impermeable, sulfhydryl-specific biotinylating reagent in intact cells expressing these mutants. The results provide experimental evidence for a topological model of a 13-transmembrane domain protein with an extracellular amino terminus and an intracellular carboxyl terminus. We also constructed a three-dimensional homology model of CHT1 based on the crystal structure of the bacterial Na<sup>+</sup>/galactose cotransporter, which supports our conclusion of CHT1 transmembrane topology. Furthermore, we examined whether CHT1 exists as a monomer or oligomer. Chemical cross-linking induces the formation of a higher molecular weight form of CHT1 on the cell surface in HEK293 cells. Two different epitope-tagged CHT1 proteins expressed in the same cells can be co-immunoprecipitated. Moreover, co-expression of an inactive mutant I89A with the wild type induces a dominant-negative effect on the overall choline uptake activity. These results indicate that CHT1 forms a homo-oligomer on the cell surface in cultured cells.

Cholinergic neurons are involved in diverse physiological, behavioral, and cognitive functions in the central and peripheral nervous system. At the cholinergic presynaptic terminals, choline is taken up from the synaptic cleft through the high-

affinity choline uptake system and is subsequently reused for acetylcholine synthesis. The high-affinity choline transporter CHT1<sup>2</sup> is responsible for this uptake (1–4), which is the rate-limiting step in acetylcholine synthesis and supports sustained acetylcholine release. Recent studies revealed that the CHT1 protein is predominantly localized at synaptic vesicles or endosomes within cholinergic nerve terminals (5–7). Heterologous expression of CHT1 in mammalian cell lines or *Xenopus* oocytes generally results in a predominant intracellular localization and very low expression of the protein in the plasma membrane, precluding detailed functional characterization of CHT1 in intact cells (5, 8–11). To date, little information is available about the structure-function relationship of CHT1.

CHT1 is a member of the SLC5 family of solute transporters and is assigned to SLC5A7 (12). Its amino acid sequence has 20–25% homology with that of other members of this family (13). It has been assumed that all members of the family possess a common 13-transmembrane domain core (14), which has been experimentally confirmed in the Na<sup>+</sup>/glucose cotransporter SGLT1 (15), bacterial Na<sup>+</sup>/proline transporter PutP (16), and Na<sup>+</sup>/iodide transporter NIS (17). A recent report of the crystal structure of a member of the SLC5 family, the *Vibrio parahaemolyticus* Na<sup>+</sup>/galactose cotransporter (vSGLT) also supports the concept of a 13-transmembrane domain core (18). Interestingly, the vSGLT protein assembles as a parallel dimer in the above crystal structure (18). Although freeze-fracture electron microscopic studies showed that SGLT1 or vSGLT functions as a monomer (19, 20), radiation inactivation studies showed that the size of the SGLT1 functional unit was estimated to be ~300 kDa, which was interpreted as evidence for a homotetramer or hetero-oligomer (21–26). Little is known about the oligomeric structure of other members of the SLC5 family.

\* This work was supported by grants from the Japan Society for the Promotion of Science and the Ministry of Education, Culture, Sports, Science, and Technology of Japan.

<sup>†</sup> To whom correspondence should be addressed. E-mail: okuda-tk@pha.keio.ac.jp or t-okuda@umin.org.

<sup>2</sup> The abbreviations used are: CHT1, high-affinity choline transporter; SLC, solute carrier family; SGLT, sodium-glucose (galactose) cotransporter; HC-3, hemicholinium-3; KRH, Krebs-Ringer-HEPES; WT, wild type; MTSEA, N-biotinylaminoethyl methanethiosulfonate; BS<sup>3</sup>, bis(sulfosuccinimidyl) suberate; SMVT, Na<sup>+</sup>/multivitamin transporter.

Here we examined the transmembrane topology of human CHT1 (hCHT1) using cysteine scanning analysis. Our results provide experimental evidence for a topological model of CHT1 as a 13-transmembrane domain protein with an extracellular amino terminus and an intracellular carboxyl terminus. We also demonstrate the existence of CHT1 homo-oligomers on the cell surface using chemical cross-linking and/or immunoprecipitation as well as functional assays after co-expression of inactive mutant versions of this protein.

## EXPERIMENTAL PROCEDURES

**DNA Constructs**—The pcDNA3.1-hCHT1 plasmid (9) was used as a template for mutagenesis. All point mutants were generated by site-directed mutagenesis (QuikChange, Stratagene), and each introduced mutation was confirmed by DNA sequencing. A plasmid encoding human Na<sup>+</sup>/multivitamin transporter (SMVT) was a kind gift from Dr. Vadivel Ganapathy (Georgia Health Sciences University). SMVT cDNA was cloned into the vector pcDNA3.1(+). For C-terminal epitope-tagged constructs, a sequence encoding the FLAG (DYKD-DDDK) or HA (YPYDVPDYA) epitope was fused to the coding region in pcDNA3.1-hCHT1 or pcDNA3.1-hSMVT.

**[<sup>3</sup>H]Choline Uptake Assay**—HEK293 cells were cultured in Dulbecco's modified Eagle's medium supplemented with 10% fetal bovine serum at 37 °C in 5% CO<sub>2</sub>. HEK293 cells stably expressing the hCHT1 WT or E451D mutant were selected by culturing in medium containing 500 μg/ml of G418 (Invitrogen). For transient expression, cells grown to ~90% confluence in 24-well culture plates were transfected with plasmid DNA (0.8 μg/well) using Lipofectamine 2000 reagent (Invitrogen) and used for uptake assays 48 h later. For co-expression of hCHT1 inactive mutants, the total DNA amount for each transfection was kept constant at 0.8 μg/well, whereas the ratios of plasmids encoding the mutant relative to the WT were changed as indicated in Fig. 6.

The choline uptake assay was performed as described previously (9). In brief, cells were preincubated with Krebs-Ringer-HEPES (KRH) buffer (130 mM NaCl, 1.3 mM KCl, 2.2 mM CaCl<sub>2</sub>, 1.2 mM MgSO<sub>4</sub>, 1.2 mM KH<sub>2</sub>PO<sub>4</sub>, 10 mM HEPES, and 10 mM glucose, pH 7.4) for 30 min at 37 °C for equilibrium. Uptake assays using 0.1 μM [<sup>3</sup>H]choline (82.0 Ci/mmol; PerkinElmer Life Sciences) were performed for 5 min at 37 °C with or without 1 μM hemicholinium-3 (HC-3). Saturation kinetics were determined using increasing concentrations of [<sup>3</sup>H]choline, with the specific activity diluted with unlabeled choline (15 Ci/mol). Uptake was terminated by three washes with ice-cold KRH buffer. Specific choline uptake was determined by subtracting the uptake in the presence of 1 μM HC-3 from the total uptake. Kinetic constants were calculated by nonlinear least-square fits (Kaleidagraph, Synergy Software). Assays were performed in triplicate and repeated at least three times.

**[<sup>3</sup>H]Hemicholinium-3 Binding Assay**—Hemicholinium-3 (HC-3) binding assays using [<sup>3</sup>H]HC-3 (125–145 Ci/mmol; PerkinElmer Life Sciences) were performed as previously described (9). In brief, cells were preincubated with KRH buffer for 30 min at 37 °C. Binding assays were performed in intact cells at 4 °C for 1 h and terminated by three washes with ice-cold KRH buffer. Except when determining saturation binding,

2 nM [<sup>3</sup>H]HC-3 was used with or without 1 μM nonlabeled HC-3 in most of the experiments. Displacement experiments were performed in intact cells incubated with 2 nM [<sup>3</sup>H]HC-3 along with various concentrations of nonlabeled choline at 4 °C.

**Biotinylation Assay**—Cells grown in 6-well culture plates were preincubated for 30 min at 37 °C in KRH buffer. Cells were treated with either *N*-biotinylaminoethyl methanethiosulfonate (MTSEA-biotin; 0.5 mM, Sigma) at 37 °C for 10 min, or sulfo-NHS-SS-Biotin (2 mM, Pierce) at 4 °C for 30 min in PBS/CM (138 mM NaCl, 2.7 mM KCl, 1.5 mM KH<sub>2</sub>PO<sub>4</sub>, 9.6 mM Na<sub>2</sub>HPO<sub>4</sub>, 0.1 mM CaCl<sub>2</sub>, and 1 mM MgCl<sub>2</sub>, pH 7.4). MTSEA-biotin and sulfo-NHS-SS-Biotin are expected to bind to -SH and -NH<sub>2</sub> groups, respectively. Unreacted biotin was removed by washing three times in PBS/calcium-magnesium. Cells were solubilized with RIPA buffer (10 mM Tris, pH 7.4, 150 mM NaCl, 1 mM EDTA, 1% Triton X-100, 0.5% deoxycholate, and 0.1% SDS) at 4 °C for 30 min. Cell lysates were centrifuged at 17,000 × *g* for 10 min at 4 °C. Biotinylated proteins were precipitated after incubation with UltraLink Plus Immobilized Streptavidin Gel (Pierce) overnight at 4 °C. The gel was washed five times with 1 ml of RIPA buffer, and proteins were eluted with SDS sample buffer (62.5 mM Tris-HCl, pH 6.8, 10% glycerol, 2% SDS, 0.1 M DTT, and 0.01% bromophenol blue). Precipitated proteins were analyzed by SDS-PAGE, followed by immunoblotting using anti-CHT1 antibody (1:2000) and an ECL detection kit (GE Healthcare).

**Homology Modeling**—The amino acid sequence of hCHT1 was initially aligned with that of vSGLT using the program DIALIGN (27), and the alignment was manually adjusted. Homology modeling of hCHT1 (amino acid sequence from residue 7 to 516) was carried out using the MODELLER 9.10 package (28), based on the atomic model of vSGLT (PDB ID code 2XQ2) (18). Energy minimization and simulated annealing were then carried out with the program CNS1.3 (29). The geometry of the constructed model was evaluated with the program PROCHECK (30), and manually corrected using the program COOT (31). These procedures were iterated several times. The models were displayed in the program PyMOL.

**Cross-linking Assay**—Cells grown in 6- or 12-well culture plates were preincubated for 30 min at 37 °C in KRH buffer. Cells were then treated with 4 mM bis(sulfosuccinimidyl) suberate (BS<sup>3</sup>, a membrane-impermeable, homobifunctional *N*-hydroxysuccinimide ester cross-linker; Pierce) in KRH at 4 °C for 120 min. For cross-linking immunoprecipitation assays, cells were treated with 4 mM BS<sup>3</sup> at 4 °C for 30 min. Unreacted BS<sup>3</sup> was quenched by incubating cells with 20 mM glycine in KRH at 4 °C for 10 min. Cells were solubilized with RIPA buffer at 4 °C for 30 min, and proteins were analyzed by SDS-PAGE, followed by immunoblotting with anti-CHT1 antibody.

**Co-immunoprecipitation Assay**—Co-immunoprecipitation assays were performed essentially as described previously (32). In brief, cells in 60-mm dishes were solubilized for 30 min with lysis buffer (1% Triton X-100, 150 mM NaCl, 1 mM EDTA, and 20 mM HEPES, pH 7.4). After centrifugation at 17,000 × *g* for 15 min, supernatants were immunoprecipitated using a monoclonal anti-FLAG-agarose-conjugated antibody (Sigma) for 1 h. Immunoprecipitates were washed with lysis buffer and eluted with SDS sample buffer. Immunoprecipitates and cell lysates

## Topology and Oligomeric Structure of Choline Transporter

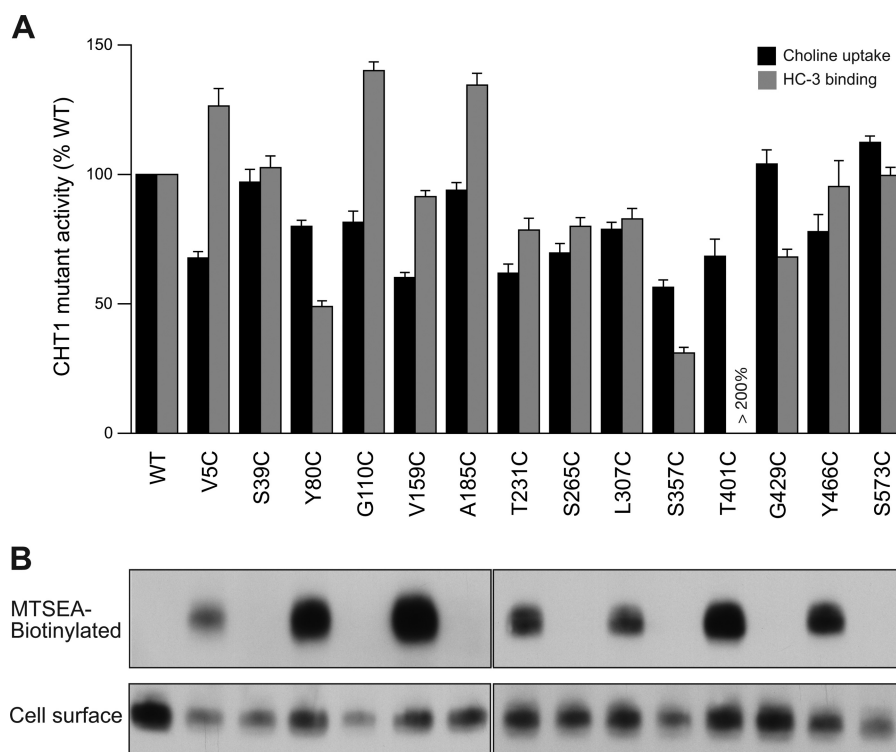


**FIGURE 1. External accessibility of hCMT1 cysteine mutants.** *A*, choline uptake and HC-3 binding activities of the mutants in HEK293 cells. The data are normalized to activity levels of the WT. HC-3 binding activity of T401C was not graphed because it was relatively high. *B*, biotinylation assays of hCMT1 cysteine mutants. MTSEA-biotin labeling of the introduced cysteine within the mutants was assessed by immunoblotting with anti-CMT1 antibody (shown as *MTSEA-biotinylated*). The cell surface expression of the mutants was monitored by biotinylation assays using membrane-impermeable sulfo-NHS-SS-biotin, which interacts with amino groups of proteins on the extracellular surface (shown below as *cell surface*).

were analyzed by SDS-PAGE, followed by immunoblotting with anti-FLAG or anti-HA antibody. Mouse monoclonal anti-FLAG (M2, Sigma) and rat monoclonal anti-HA (3F10, Roche Applied Science) were the primary antibodies.

**Statistics**—Data are presented as mean  $\pm$  S.E. Statistical significance was determined by unpaired Student's *t* test.

### RESULTS

To examine the transmembrane topology of hCMT1 by cysteine-scanning analysis, we first generated a cysteine-less mutant of hCMT1 to provide a background in which all five of the endogenous cysteine residues were replaced by serine. However, this mutant is nonfunctional when expressed in HEK293 cells (data not shown). Therefore, we assessed the external accessibility of the five endogenous cysteine residues of hCMT1. HEK293 cells were transfected with hCMT1, and intact cells were treated with MTSEA-biotin. MTSEA is a membrane-impermeable sulfhydryl reagent that reacts only with cysteine residues on the external surface of the cells. Thus, if intact cells are incubated with an excess of MTSEA, cysteine residues exposed to the outside will react with this compound. Because it labels cysteine residues with a biotin moiety, labeled proteins can be selectively purified from cell lysates using an avidin-conjugated gel. The MTSEA-biotin reactivity of hCMT1 was assessed by immunoblotting of the precipitated proteins with anti-CMT1 antibody. Under our biotinylation conditions, no labeling was observed for hCMT1 (Fig. 1*B*, *left*), suggesting that endogenous cysteine residues are inaccessible from the extracellular side. Significant labeling was observed only when

cells were permeabilized with a detergent such as saponin or digitonin prior to labeling (data not shown).

We next introduced a single cysteine residue into various positions in the predicted extracellular or intracellular regions to assess the external accessibility. These residues cover all the putative hydrophilic regions, including the amino- and carboxyl-terminal tails of hCMT1. We measured both choline uptake and HC-3 binding activities of all these mutants. A hydrophilic ligand HC-3 contains quaternary nitrogens and is used to assess the CMT1 expression level on the cell surface. The cell surface expression level was also assessed by cell surface biotinylation assays as described below, in case that some mutations might cause the loss of HC-3 binding activity without affecting the cell surface expression. The mutants were selected so that they retain both choline uptake and HC-3 binding activities to at least 30% of that of the wild type (WT) when expressed in HEK293 cells (V5C, S39C, Y80C, G110C, V159C, A185C, T231C, S265C, L307C, S357C, T401C, G429C, Y466C, and S573C) (Fig. 1*A*).

We examined the MTSEA-biotin labeling of the introduced cysteine within each mutant in intact cells. Biotin labeling was detected for cysteine residues introduced at positions 5, 80, or 159 (Fig. 1*B*, *upper*). The labeling was also observed, albeit to a lesser extent, for cysteines at positions 231, 307, 401, or 466. In contrast, no labeling was observed for cysteine residues within the WT or cysteines introduced at positions 39, 110, 185, 265, 357, 429, or 573, under the same conditions (Fig. 1*B*, *upper*). All the mutants could be labeled with a membrane-impermeable

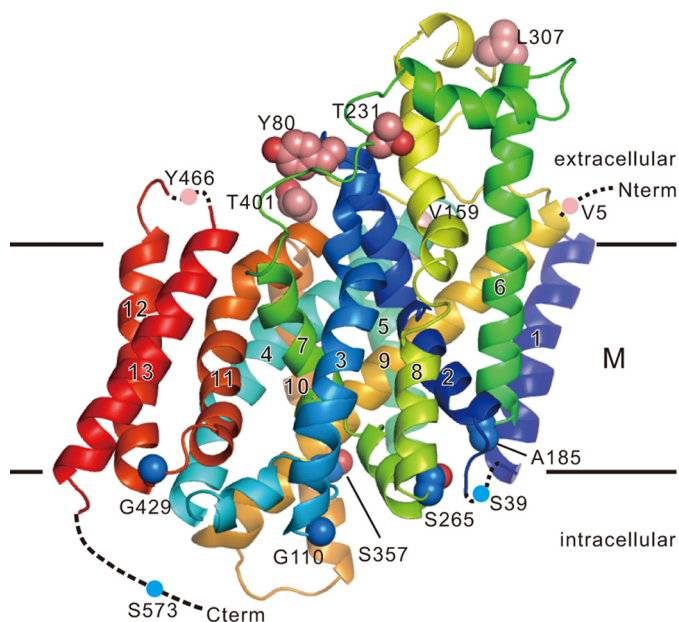


**FIGURE 2. hCMT1 homology model based on the vSGLT structure.** Ribbon representation of the constructed model of hCMT1, in which  $\alpha$ -helices are numbered. Horizontal bars represent the boundaries of the hydrophobic core of the lipid bilayer (M: membrane). Color changes gradually from the amino terminus (N, blue) to the carboxyl terminus (C, red). The unmodeled loops and carboxyl terminus are represented by dotted and a dashed line, respectively. The residues examined by MTSEA-biotin labeling in Fig. 1 are represented by space filling model. Carbon atoms of amino acid residues that are extracellularly accessible or inaccessible are shown in pink or cyan, respectively. Oxygen atoms are shown in red. The accessible or inaccessible residues located on unmodeled regions are represented by circles in pink or cyan, respectively.

reagent, sulfo-NHS-SS-biotin, which labels amino groups of proteins on the cell surface (Fig. 1B, lower). These results indicate that at least seven residues, Val-5, Tyr-80, Val-159, Thr-231, Leu-307, Thr-401, and Tyr-466, when mutated to cysteine, are accessible from the external medium, and thus expected to be located in extracellular regions of hCMT1. Taken together, these results provide experimental evidence for a topological model of hCMT1 as a 13-transmembrane domain protein with an extracellular amino terminus and an intracellular carboxyl terminus (Fig. 2).

Recently, the crystal structure of vSGLT, a member of the SLC5 family, was reported (18), and we constructed a three-dimensional homology model of hCMT1 based on the vSGLT structure (Fig. 2). In this model, the residues labeled with MTSEA-biotin are located extracellularly; the unlabeled residues are located intracellularly, further supporting our conclusion of hCMT1 transmembrane topology (Fig. 2).

We next focused on the oligomeric structure of CHT1. To explore the possibility that CHT1 may exist as an oligomer, we used a membrane-impermeable, homobifunctional *N*-hydroxysuccinimide ester cross-linker, BS<sup>3</sup>, capable of cross-linking near lysine residues on the cell surface, to treat intact HEK293 cells stably expressing hCMT1. After chemical cross-linking, cells were solubilized and proteins were analyzed by immunoblotting with an anti-CHT1 antibody. As shown in Fig. 3A, treatment of cells with BS<sup>3</sup> resulted in unique bands with a high molecular weight. The prominent cross-linked bands migrating at ~120 kDa are likely to represent the hCMT1 homodimer. Oligomers of hCMT1 were detected after cross-

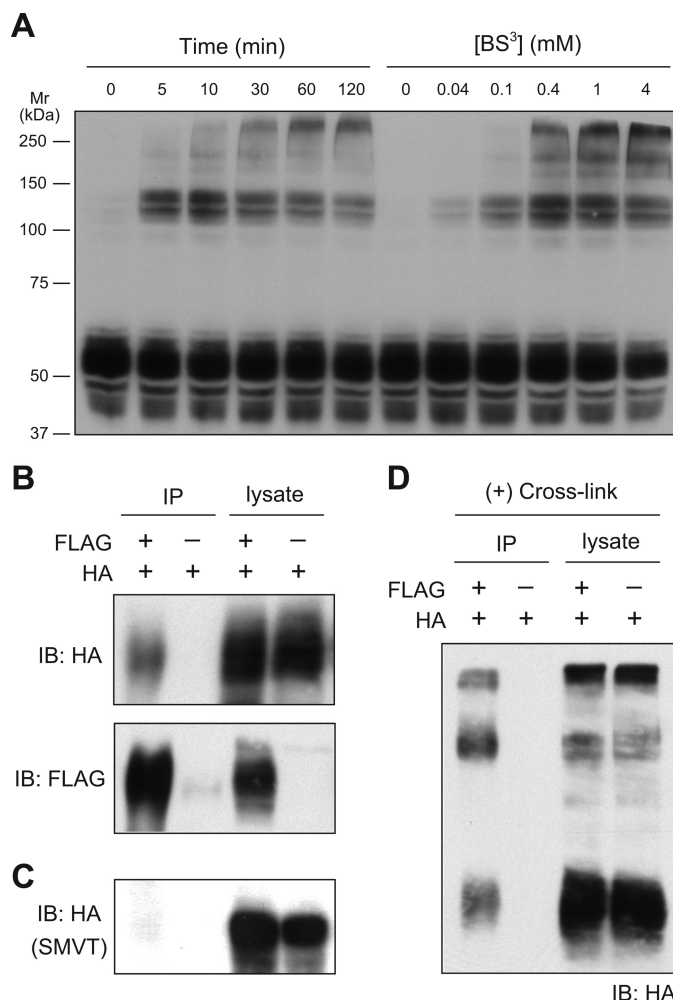


**FIGURE 3. Characterization of hCMT1 oligomers.** A, cross-linking of cell surface proteins in hCMT1-expressing HEK293 cells using a cross-linker, BS<sup>3</sup>. Cells were treated with 4 mM BS<sup>3</sup> at 4°C for the indicated time (left) or with the indicated concentration of BS<sup>3</sup> for 120 min (right). Cells were lysed after cross-linking and cell lysates were immunoblotted (IB) with anti-CHT1 antibody. B, co-immunoprecipitation assay using two different versions of epitope-tagged CHT1. Lysates from cells expressing CHT1-FLAG and/or CHT1-HA were precipitated by anti-FLAG antibody and immunoblotted with anti-HA or anti-FLAG antibody. The input lanes represent 10% of cell lysates used in the co-immunoprecipitation assays (shown as lysate). C, co-immunoprecipitation assay using CHT1 and SMVT. Lysates from cells expressing CHT1-FLAG and/or SMVT-HA were precipitated by anti-FLAG antibody and immunoblotted with anti-HA antibody. D, cross-linking immunoprecipitation assay. Cells expressing CHT1-FLAG and/or CHT1-HA were first cross-linked with 4 mM BS<sup>3</sup> at 4°C for 30 min, after which cell lysates were precipitated by anti-FLAG antibody as in B. The input lanes represent 10% of cell lysates used in the co-immunoprecipitation (shown as lysate).

linking by BS<sup>3</sup> in a time- and dose-dependent manner (Fig. 3A). Those bands were not detected in cell lysates from nontreated cells; in these lysates only monomeric bands (~55 kDa) were detected ("0" in Fig. 3A). This finding raises the possibility that CHT1 exists as an oligomer at the cell surface.

In the above cross-linking experiment, it was possible that CHT1 may have been cross-linked with an unknown CHT1-associated protein. To eliminate this possibility and to confirm that the observed ~120-kDa band is indeed homomeric CHT1, we used two different epitope-tagged hCMT1 proteins for co-immunoprecipitation assays. HEK293 cells were simultaneously transfected with a construct expressing FLAG-tagged

## Topology and Oligomeric Structure of Choline Transporter

CHT1 (CHT1-FLAG) and a construct expressing HA-tagged CHT1 (CHT1-HA). CHT1-FLAG was then precipitated from the cell lysate by an anti-FLAG antibody, and the precipitates were analyzed by immunoblotting with an anti-HA antibody. As shown in Fig. 3B, CHT1-HA was specifically detected in the anti-FLAG precipitates, which was not detected in the anti-FLAG precipitates from the lysate prepared from cells expressing CHT1-HA only. When cells were simultaneously transfected with CHT1-FLAG and HA-tagged Na<sup>+</sup>/multivitamin transporter (SMVT-HA, another member of SLC5 family), SMVT-HA was not detected in the anti-FLAG precipitates, suggesting that our co-immunoprecipitation assay was specific to CHT1 homo-oligomers (Fig. 3C). Furthermore, when the co-immunoprecipitation assay was performed after cross-linking with BS<sup>3</sup>, specific cross-linked CHT1-HA signals were detected in the anti-FLAG precipitates (Fig. 3D). These results indicate that the oligomer observed in the above cross-linking assays contains a CHT1 homo-oligomer, suggesting that CHT1 exists as a homo-oligomer at the cell surface.

If two or more monomers form the functional transporter for CHT1, then the presence of an inactive mutant along with the WT could decrease the overall choline uptake activity. In an attempt to obtain an inactive mutant, we mutated negatively charged residues located within or proximal to the transmembrane regions of hCHT1. It is possible that negatively charged residues would be involved in the transport of Na<sup>+</sup> and choline. We generated a series of 11 mutants, in each of which a single residue (Asp or Glu) had been replaced with a noncharged residue (Asn or Gln) by site-directed mutagenesis (mutants: E6Q, D48N, E138Q, D158N, D160N, D188N, E236Q, D242N, D349N, D411N, and E451Q). The positions of these residues in the hCHT1 structure model are shown in Fig. 4A. Each of these mutants was transiently expressed in HEK293 cells. Immunoblot analysis showed that mutants D48N, D242N, and D411N were not efficiently expressed (Fig. 4B).

We measured both choline uptake and HC-3 binding activities of all these mutants. The mutants E6Q, D158N, D160N, and E236Q had comparable levels of choline uptake and HC-3 binding activities with the WT (Fig. 4C). The mutants E138Q, D188N, and D349N completely lost both choline uptake and HC-3 binding activities, despite their expression on the cell surface, as shown by the cell surface biotinylation assay, indicating that they lost ligand binding activity (Fig. 4B). The mutant E451Q demonstrated impaired choline uptake activity without a concomitant change in its HC-3 binding activity (Fig. 4C). Kinetic analysis of the HC-3 binding activity showed that E451Q had a slightly higher affinity for HC-3 (data not shown). We next introduced a conservative change at this position (E451D) and measured choline uptake activity of the mutant. Choline uptake activity of E451D was still lower than that of the WT, and thus, analysis was hereafter focused on E451D.

We generated stable HEK293 cell lines expressing either the WT or E451D. Several cell lines were obtained, and a cell surface biotinylation assay was performed for each line. The cell lines that showed similar expression levels on the cell surface were chosen as representatives of the WT and E451D (Fig. 5A). Kinetic analysis of choline uptake revealed that the mutant E451D showed ~3-fold reduction in the apparent affinity for

choline, without a significant change in  $V_{\max}$  (Fig. 5B). The  $K_m$  value for choline was  $3.3 \pm 0.2 \mu\text{M}$  for the WT and  $10.5 \pm 1.5 \mu\text{M}$  for E451D ( $p < 0.01$ ,  $n = 3$ ), and the  $V_{\max}$  value was  $1.6 \pm 0.1$  for the WT and  $1.7 \pm 0.1$  (nmol/min/mg protein) for E451D ( $p > 0.5$ ,  $n = 3$ ). In contrast, saturation analysis of HC-3 binding revealed that the E451D mutant had a ~3-fold increase in the apparent affinity for HC-3 (Fig. 5B). The  $K_d$  value for HC-3 was  $15.6 \pm 1.3 \text{ nM}$  for the WT and  $5.0 \pm 0.1 \text{ nM}$  for E451D ( $p < 0.01$ ,  $n = 3$ ). To estimate the apparent binding affinity of E451D for choline, a [<sup>3</sup>H]HC-3 binding assay was performed with increasing concentrations of nonlabeled choline. The [<sup>3</sup>H]HC-3 binding for E451D was displaced by a higher concentration of choline than that required for the WT (Fig. 5C). Consistent with the result from kinetic analysis of choline uptake, E451D showed an ~6-fold reduction in the binding affinity for choline. Given the  $\text{IC}_{50}$  value for choline ( $0.9 \pm 0.1 \mu\text{M}$  for the WT;  $7.1 \pm 0.3 \mu\text{M}$  for E451D), the  $K_i$  value for choline was calculated to be  $0.81 \pm 0.1 \mu\text{M}$  for WT and  $5.2 \pm 0.2 \mu\text{M}$  for E451D ( $p < 0.01$ ,  $n = 3$ ). We concluded that residue Glu-451 in transmembrane domain 12 is important for substrate recognition in CHT1, and E451Q could be considered as a mutant deficient in substrate binding.

To examine the functional impact of co-expression with inactive mutants, we utilized two mutants, I89A and E451Q (Fig. 6A), both of which demonstrated significant loss of choline uptake activity (I89A and E451Q; ~20 and 5%, compared with the WT, respectively). I89A located within transmembrane domain 3 showed an impaired choline transport rate without significant changes in its affinity for choline, and is considered to have a deficit in substrate translocation and consequently has a lower turnover rate (9). Transmembrane domain 3 of vSGLT was suggested to show a large structural rearrangement during substrate translocation (18). In contrast, E451Q located within transmembrane domain 12 has a replacement of functionally important amino acids for choline binding, as exemplified in the above results of E451D (Figs. 4 and 5). The positions of these residues in the structure model are shown in Fig. 6A. Both mutants show a slightly higher affinity for HC-3, but had similar expression levels on the cell surface. We first confirmed that both mutants tagged with HA could be co-immunoprecipitated by WT CHT1-FLAG, indicating that they are capable of forming homo-oligomers (Fig. 6B). Next, we co-expressed the inactive mutants with the WT in HEK293 cells, and analyzed both choline uptake and HC-3 binding activities. Each transfection was performed with a constant amount of plasmid DNA, in which the ratio of the mutant to the WT was changed. As shown in Fig. 6C, co-expression of I89A showed a dominant-negative effect on choline uptake activity. This effect was not accompanied by alteration in the expression level on the cell surface, as assessed by HC-3 binding activity (Fig. 6C). However, no dominant-negative effect was observed for co-expression of E451Q, in which choline uptake activity was reduced linearly with increasing ratios of the mutant to the WT (Fig. 6C, right). These results suggest that oligomers can be formed between the mutants and the WT on the cell surface, and that the mutant I89A, but not E451Q, consequently affects the overall choline uptake rate of CHT1.

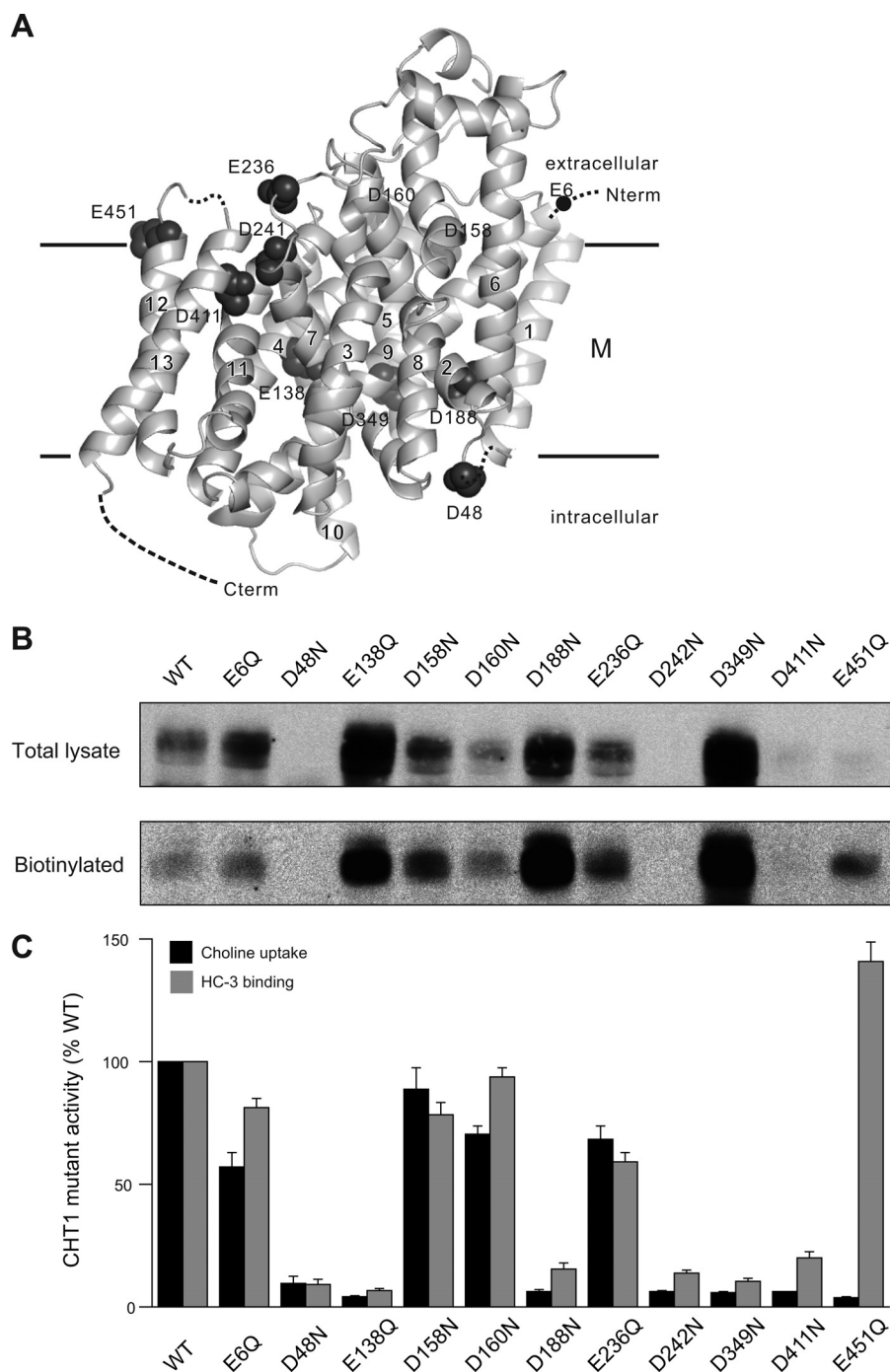


**FIGURE 4. Functional characterization of hCht1 mutants with altered negatively charged residues.** *A*, the positions of 11 negatively charged residues mutated in this study are indicated in space filling model within the constructed model. *B*, cell surface biotinylation assay of the mutants. Cells expressing each mutant were labeled with membrane-impermeable, sulfo-NHS-SS-biotin, and biotinylated proteins were immunoblotted with streptavidin gel. Precipitated proteins (*Biotinylated*) or cell lysate (*Total lysate*) were immunoblotted with anti-Cht1 antibody. The mutants D48N, D242N, and D411N are not efficiently expressed in cells, possibly because these residues are required for proper trafficking to the cell membrane. *C*, choline uptake and HC-3 binding activities of the mutants in HEK293 cells. The data are normalized to activity levels of the WT.

## DISCUSSION

Using cysteine scanning analysis, we examined the transmembrane topology of hCht1, a member of the SLC5 family. Our results provide the first experimental evidence for a topological model of Cht1 as a 13-transmembrane domain protein with an extracellular amino terminus and an intracellular carboxyl terminus. The amino terminus of Cht1 has been previously demonstrated to be located extracellularly by immuno-

fluorescence analysis, in which an amino-terminal FLAG-tagged protein was detected by a FLAG antibody in live cells (10, 33). The overall result is consistent with reports of other members of this family, such as the Na<sup>+</sup>/glucose cotransporter SGLT1 (15–17), suggesting that all members of the family possess a common 13-transmembrane domain core (14). The recent report of the crystal structure of vSGLT also supports the concept of a 13-transmembrane domain core (18).

## Topology and Oligomeric Structure of Choline Transporter

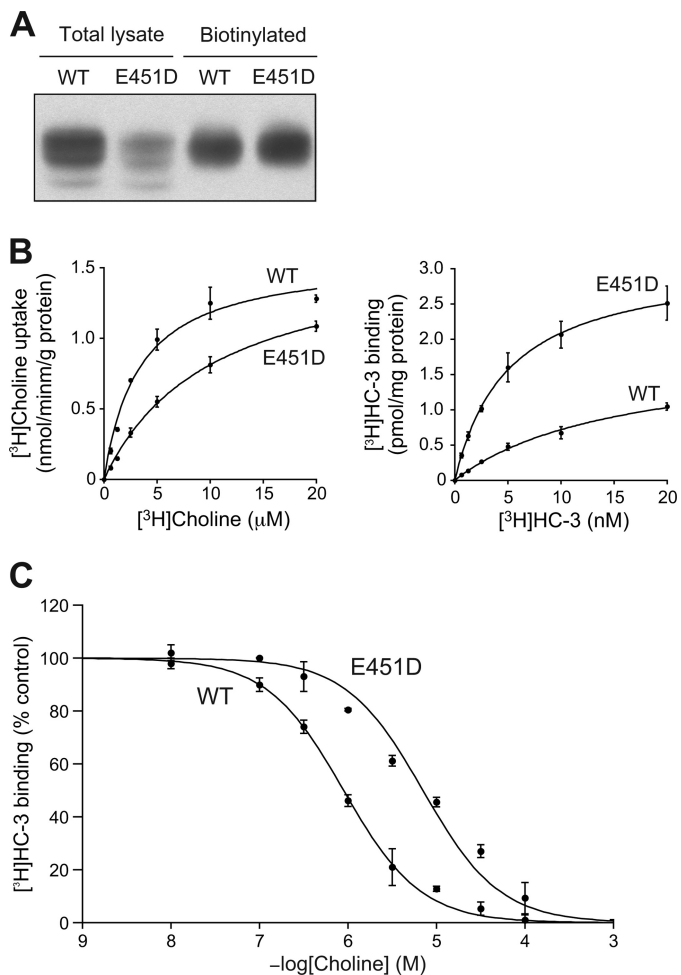


**FIGURE 5. Functional properties of hCMT1 E451D mutant.** *A*, cell surface biotinylation assay using stable cell lines expressing the WT or E451D. Biotinylated proteins were prepared from 5-fold the amount of total lysate loaded on the gel. *B*, saturation analysis of [ $^3$ H]choline uptake (shown *left*) and [ $^3$ H]HC-3 binding activities (*right*) of the WT and E451D. *C*, the displacement of [ $^3$ H]HC-3 binding by nonlabeled choline in intact cells expressing either the WT or E451D. The data are normalized to [ $^3$ H]HC-3 binding in the absence of nonlabeled choline.

CHT1 contains several charged residues predicted to reside within the transmembrane domains. Here we also report roles of negatively charged residues located within or proximal to the transmembrane domains. We especially focused on Glu-451 within transmembrane domain 12. Functional analysis of mutants E451D and E451Q suggested that a negative charge is required at position 451, and Glu-451 may be involved in substrate binding of CHT1. However, Glu-451 is located outside the substrate-binding site in the structure model (Figs. 4A and 6A), assuming that the choline binding site is located in the same position as the galactose binding site of vSGLT (18). It is likely that Glu-451 is involved in substrate binding of CHT1 indirectly through maintenance of structural integrity, although it remains to be elucidated how Glu-451 is involved in it.

We provide several independent lines of evidence to support the concept that CHT1 forms a homo-oligomer at the cell surface when expressed in cultured cells. First, chemical cross-linking analysis revealed the existence of CHT1 oligomers at the cell surface. Second, two different epitope-tagged CHT1

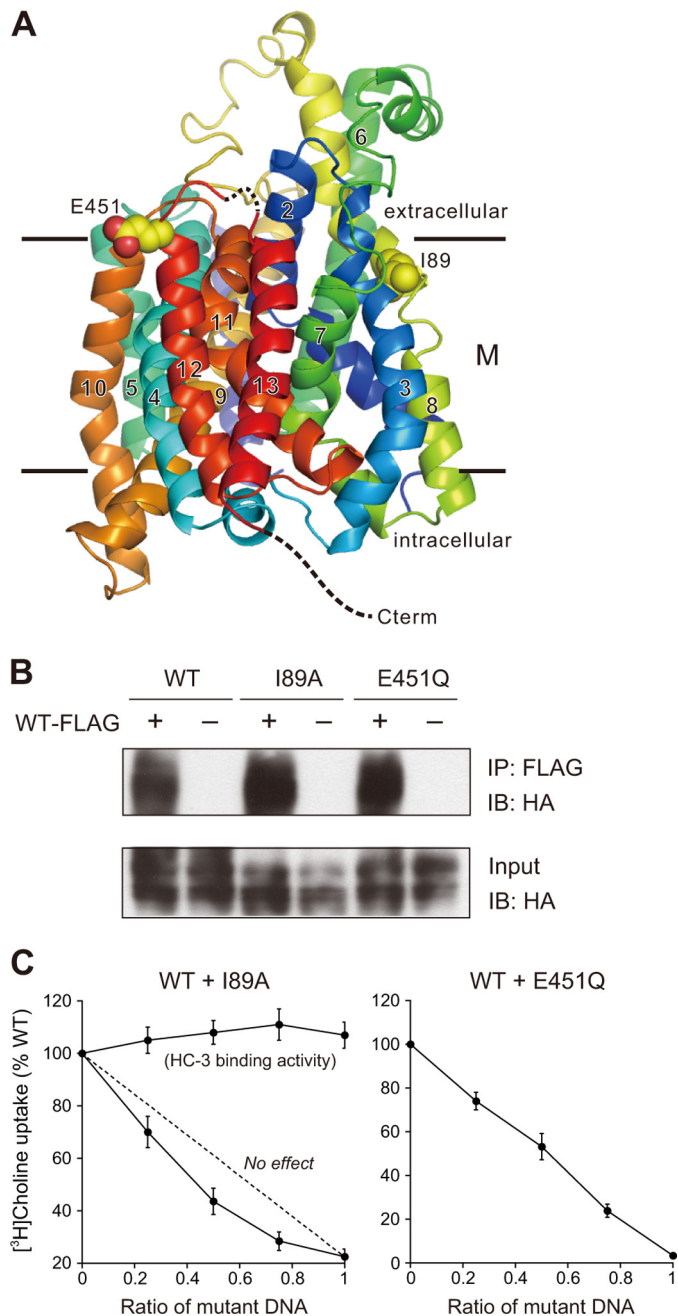


**FIGURE 6. Dominant-negative effect by co-expression of an inactive mutant of CHT1 on the choline uptake activity of the WT.** *A*, the positions of Ile-189 and Glu-451 are indicated in space filling model within the constructed model. Carbon and oxygen atoms are shown in yellow and red, respectively. The molecule is rotated by 90° from the orientation of the model in Figs. 2 and 4A. *B*, co-immunoprecipitation (IP) assay. For CHT1 WT, I89A, and E451Q, lysates from cells co-expressing CHT1-FLAG (WT) and CHT1-HA (WT or each mutant) were precipitated by anti-FLAG antibody, and the precipitates were immunoblotted (IB) with anti-HA or anti-FLAG antibody. The *input* lanes represent 10% of cell lysates used in the immunoprecipitation. *C*, dominant-negative effect by co-expression of the inactive hCMT1 mutant. Various ratios of plasmids encoding hCMT1 mutant (I89A or E451Q) relative to the WT were co-transfected into HEK293 cells, whereas the total DNA amount for each transfection was kept constant. The cells were assayed for [ $^3$ H]choline uptake and [ $^3$ H]HC-3 binding activities. The data are normalized to activity of cells transfected with the WT only. For the HC-3 binding activity of I89A, 5 nM [ $^3$ H]HC-3 was used in the binding assay.

proteins expressed in the same cells could be co-immunoprecipitated, and this co-immunoprecipitation could be similarly observed with the cross-linked CHT1 proteins on the cell sur-

face. Third, co-expression of an inactive mutant I89A with the WT induced a dominant-negative effect on the overall choline uptake activity of CHT1, suggesting that oligomers can be formed between the mutant I89A and WT at the cell surface, and that the mutant consequently affects the overall choline uptake activity of CHT1. This effect did not result from a reduced expression level of the WT at the plasma membrane, as revealed by HC-3 binding assays. Rather, it can be assumed that the dominant-negative effect is caused by a reduced turnover rate of the oligomers formed between I89A and WT on the cell surface.

It appears that the dominant-negative effect of I89A co-expression supports the concept that homo-oligomerization is essential for CHT1 function. However, this is inconsistent with the results of co-expression of the inactive mutant E451Q, in which no dominant-negative effect was observed. Instead, the result from E451Q co-expression supports the concept that each CHT1 monomer within the homo-oligomer can function independently of the other monomer(s). The lack of a dominant-negative effect by co-expression of a WT and an inactive mutant protein has been reported for other homo-oligomeric transporters, such as Na<sup>+</sup>/H<sup>+</sup> exchanger 1 (34), renal type IIa Na<sup>+</sup>/P<sub>i</sub> cotransporter (35), and reduced folate carrier (36). It remains to be elucidated how I89A, and not the E451Q monomer, impairs substrate translocation or reorientation of the WT monomer via oligomerization.

CHT1 is a member of the SLC5 family, and our preliminary results also reveal the existence of homo-oligomers in SGLT1 or SMVT, other members of SLC5 family, as analyzed by chemical cross-linking and co-immunoprecipitation assays in HEK293 cells.<sup>3</sup> The recent report on the vSGLT structure showed that the vSGLT protein was assembled as a parallel dimer in the crystal structure (18), a finding that is consistent with our results. Although freeze-fracture electron microscopic studies showed that SGLT1 was a monomer (19, 20), radiation inactivation studies showed that the size of the SGLT1 functional unit was estimated to be that of a homotetramer (21–26). Interestingly, members of SLC5 share a highly conserved GXXXG motif within transmembrane domain 12. The GXXXG motif, which has been shown to be critical for homodimerization of some proteins, is a frequently occurring sequence motif for transmembrane helix-helix association (37). We transfected HEK293 cells with hCHT1 mutants in which the respective glycine residue (Gly-434, Gly-438, or Gly-442) had been replaced by a bulky hydrophobic residue, such as leucine, but these mutants could not be efficiently expressed in the cells.<sup>3</sup> It is tempting to speculate that the conserved GXXXG motif is essential for homo-oligomerization and proper trafficking of SLC5 transporters to the cell membrane.

There is a functionally relevant, nonsynonymous single nucleotide polymorphism in the *hCHT1* gene (265A>G, rs1013940) that results in an isoleucine to valine substitution (I89V) within transmembrane domain 3 of the protein (9). The I89V variant transporter shows a 40–50% decrease in the choline uptake rate compared with that of the WT *in vitro*. This

polymorphism was recently reported to be associated with major depressive disorder (38) and attention-deficit hyperactivity disorder (39). This association could be partly explained by an assumption that the I89V variant transporter has a dominant-negative effect on choline uptake activity through homo-oligomerization. In fact, some coding variants in other transporters are known to act dominantly, which could be explained by a dominant-negative interaction (40, 41). This CHT1 polymorphism may have a significant impact on choline uptake function by means of dominant-negative interaction *in vivo*.

*Acknowledgments*—We thank Dr. Vadivel Ganapathy for gifting a SMVT plasmid and China Kaitsuka for providing technical assistance.

## REFERENCES

- Okuda, T., and Haga, T. (2003) High-affinity choline transporter. *Neurochem. Res.* **28**, 483–488
- Ferguson, S. M., and Blakely, R. D. (2004) The choline transporter resurfaces. New roles for synaptic vesicles? *Mol. Interv.* **4**, 22–37
- Sarter, M., and Parikh, V. (2005) Choline transporters, cholinergic transmission and cognition. *Nat. Rev. Neurosci.* **6**, 48–56
- Ribeiro, F. M., Black, S. A., Prado, V. F., Rylett, R. J., Ferguson, S. S., and Prado, M. A. (2006) The “ins” and “outs” of the high-affinity choline transporter CHT1. *J. Neurochem.* **97**, 1–12
- Ribeiro, F. M., Alves-Silva, J., Volkmandt, W., Martins-Silva, C., Mahmud, H., Wilhelm, A., Gomez, M. V., Rylett, R. J., Ferguson, S. S., Prado, V. F., and Prado, M. A. (2003) The hemicholinium-3 sensitive high affinity choline transporter is internalized by clathrin-mediated endocytosis and is present in endosomes and synaptic vesicles. *J. Neurochem.* **87**, 136–146
- Ferguson, S. M., Savchenko, V., Apparsundaram, S., Zwick, M., Wright, J., Heilman, C. J., Yi, H., Levey, A. I., and Blakely, R. D. (2003) Vesicular localization and activity-dependent trafficking of presynaptic choline transporters. *J. Neurosci.* **23**, 9697–9709
- Nakata, K., Okuda, T., and Misawa, H. (2004) Ultrastructural localization of high-affinity choline transporter in the rat neuromuscular junction. Enrichment on synaptic vesicles. *Synapse* **53**, 53–56
- Okuda, T., and Haga, T. (2000) Functional characterization of the human high-affinity choline transporter. *FEBS Lett.* **484**, 92–97
- Okuda, T., Okamura, M., Kaitsuka, C., Haga, T., and Gurwitz, D. (2002) Single nucleotide polymorphism of the human high affinity choline transporter alters transport rate. *J. Biol. Chem.* **277**, 45315–45322
- Ribeiro, F. M., Black, S. A., Cregan, S. P., Prado, V. F., Prado, M. A., Rylett, R. J., and Ferguson, S. S. (2005) Constitutive high-affinity choline transporter endocytosis is determined by a carboxyl-terminal tail dileucine motif. *J. Neurochem.* **94**, 86–96
- Iwamoto, H., Blakely, R. D., and De Felice, L. J. (2006) Na<sup>+</sup>, Cl<sup>-</sup>, and pH dependence of the human choline transporter (hCHT) in *Xenopus* oocytes. The proton inactivation hypothesis of hCHT in synaptic vesicles. *J. Neurosci.* **26**, 9851–9859
- Wright, E. M., and Turk, E. (2004) The sodium/glucose cotransport family SLC5. *Pflugers Arch.* **447**, 510–518
- Okuda, T., Haga, T., Kanai, Y., Endou, H., Ishihara, T., and Katsura, I. (2000) Identification and characterization of the high-affinity choline transporter. *Nat. Neurosci.* **3**, 120–125
- Turk, E., and Wright, E. M. (1997) Membrane topology motifs in the SGLT cotransporter family. *J. Membr. Biol.* **159**, 1–20
- Turk, E., Kerner, C. J., Lostao, M. P., and Wright, E. M. (1996) Membrane topology of the human Na<sup>+</sup>/glucose cotransporter SGLT1. *J. Biol. Chem.* **271**, 1925–1934
- Jung, H., Rübénhagen, R., Tebbe, S., Leifker, K., Tholema, N., Quick, M., and Schmid, R. (1998) Topology of the Na<sup>+</sup>/proline transporter of *Escherichia coli*. *J. Biol. Chem.* **273**, 26400–26407
- Levy, O., De la Vieja, A., Ginter, C. S., Riedel, C., Dai, G., and Carrasco, N.

<sup>3</sup> T. Okuda, unpublished observations.

## Topology and Oligomeric Structure of Choline Transporter

- (1998) N-Linked glycosylation of the thyroid  $\text{Na}^+/\text{I}^-$  symporter (NIS). Implications for its secondary structure model. *J. Biol. Chem.* **273**, 22657–22663
18. Faham, S., Watanabe, A., Besserer, G. M., Cascio, D., Specht, A., Hirayama, B. A., Wright, E. M., and Abramson, J. (2008) The crystal structure of a sodium galactose transporter reveals mechanistic insights into  $\text{Na}^+$ /sugar symport. *Science* **321**, 810–814
  19. Eskandari, S., Wright, E. M., Kreman, M., Starace, D. M., and Zampighi, G. A. (1998) Structural analysis of cloned plasma membrane proteins by freeze-fracture electron microscopy. *Proc. Natl. Acad. Sci. U.S.A.* **95**, 11235–11240
  20. Turk, E., Kim, O., le Coutre, J., Whitelegge, J. P., Eskandari, S., Lam, J. T., Kreman, M., Zampighi, G., Faull, K. F., and Wright, E. M. (2000) Molecular characterization of *Vibrio parahaemolyticus* vSGLT. A model for sodium-coupled sugar cotransporters. *J. Biol. Chem.* **275**, 25711–25716
  21. Lin, J. T., Szwarc, K., Kinne, R., and Jung, C. Y. (1984) Structural state of the  $\text{Na}^+/\text{D}$ -glucose cotransporter in calf kidney brush-border membranes. Target size analysis of  $\text{Na}^+$ -dependent phlorizin binding and  $\text{Na}^+$ -dependent D-glucose transport. *Biochim. Biophys. Acta* **777**, 201–208
  22. Takahashi, M., Malathi, P., Preiser, H., and Jung, C. Y. (1985) Radiation inactivation studies on the rabbit kidney sodium-dependent glucose transporter. *J. Biol. Chem.* **260**, 10551–10556
  23. Béliveau, R., Demeule, M., Ibnoul-Khatib, H., Bergeron, M., Beaugerard, G., and Potier, M. (1988) Radiation-inactivation studies on brush-border membrane vesicles. General considerations, and application to the glucose and phosphate carriers. *Biochem. J.* **252**, 807–813
  24. Stevens, B. R., Fernandez, A., Hirayama, B., Wright, E. M., and Kempner, E. S. (1990) Intestinal brush-border membrane  $\text{Na}^+/\text{glucose}$  cotransporter functions *in situ* as a homotetramer. *Proc. Natl. Acad. Sci. U.S.A.* **87**, 1456–1460
  25. Koepsell, H., and Spangenberg, J. (1994) Function and presumed molecular structure of  $\text{Na}^+/\text{D}$ -glucose cotransport systems. *J. Membr. Biol.* **138**, 1–11
  26. Jetté, M., Vachon, V., Potier, M., and Béliveau, R. (1997) Radiation-inactivation analysis of the oligomeric structure of the renal sodium/D-glucose symporter. *Biochim. Biophys. Acta* **1327**, 242–248
  27. Morgenstern, B. (2004) DIALIGN: multiple DNA and protein sequence alignment at BiBiServ. *Nucleic Acids Res.* **32**, W33–36
  28. Sali, A., and Blundell, T. L. (1993) Comparative protein modelling by satisfaction of spatial restraints. *J. Mol. Biol.* **234**, 779–815
  29. Brünger, A. T., Adams, P. D., Clore, G. M., DeLano, W. L., Gros, P., Grosse-Kunstleve, R. W., Jiang, J. S., Kuszewski, J., Nilges, M., Pannu, N. S., Read, R. J., Rice, L. M., Simonson, T., and Warren, G. L. (1998) Crystallography & NMR system. A new software suite for macromolecular structure determination. *Acta Crystallogr. D Biol. Crystallogr.* **54**, 905–921
  30. Laskowski, R. A., Moss, D. S., and Thornton, J. M. (1993) Main-chain bond lengths and bond angles in protein structures. *J. Mol. Biol.* **231**, 1049–1067
  31. Emsley, P., and Cowtan, K. (2004) Coot. Model-building tools for molecular graphics. *Acta Crystallogr. D Biol. Crystallogr.* **60**, 2126–2132
  32. Okuda, T., Yu, L. M., Cingolani, L. A., Kemler, R., and Goda, Y. (2007)  $\beta$ -Catenin regulates excitatory postsynaptic strength at hippocampal synapses. *Proc. Natl. Acad. Sci. U.S.A.* **104**, 13479–13484
  33. Okuda, T., Konishi, A., Misawa, H., and Haga, T. (2011) Substrate-induced internalization of the high-affinity choline transporter. *J. Neurosci.* **31**, 14989–14997
  34. Fafournoux, P., Noël, J., and Pouységur, J. (1994) Evidence that  $\text{Na}^+/\text{H}^+$  exchanger isoforms NHE1 and NHE3 exist as stable dimers in membranes with a high degree of specificity for homodimers. *J. Biol. Chem.* **269**, 2589–2596
  35. Köhler, K., Forster, I. C., Lambert, G., Biber, J., and Murer, H. (2000) The functional unit of the renal type IIa  $\text{Na}^+/\text{P}_i$  cotransporter is a monomer. *J. Biol. Chem.* **275**, 26113–26120
  36. Hou, Z., Cherian, C., Drews, J., Wu, J., and Matherly, L. H. (2010) Identification of the minimal functional unit of the homo-oligomeric human reduced folate carrier. *J. Biol. Chem.* **285**, 4732–4740
  37. Russ, W. P., and Engelman, D. M. (2000) The GxxxG motif: a framework for transmembrane helix-helix association. *J. Mol. Biol.* **296**, 911–919
  38. Hahn, M. K., Blackford, J. U., Haman, K., Mazei-Robison, M., English, B. A., Prasad, H. C., Steele, A., Hazelwood, L., Fentress, H. M., Myers, R., Blakely, R. D., Sanders-Bush, E., and Shelton, R. (2008) Multivariate permutation analysis associates multiple polymorphisms with subphenotypes of major depression. *Genes Brain Behav.* **7**, 487–495
  39. English, B. A., Hahn, M. K., Gizer, I. R., Mazei-Robison, M., Steele, A., Kurnik, D. M., Stein, M. A., Waldman, I. D., and Blakely, R. D. (2009) Choline transporter gene variation is associated with attention-deficit hyperactivity disorder. *J. Neurodev. Disord.* **1**, 252–263
  40. Trotti, D., Aoki, M., Pasinelli, P., Berger, U. V., Danbolt, N. C., Brown, R. H., Jr., and Hediger, M. A. (2001) Amyotrophic lateral sclerosis-linked glutamate transporter mutant has impaired glutamate clearance capacity. *J. Biol. Chem.* **276**, 576–582
  41. Hahn, M. K., Robertson, D., and Blakely, R. D. (2003) A mutation in the human norepinephrine transporter gene (SLC6A2) associated with orthostatic intolerance disrupts surface expression of mutant and wild-type transporters. *J. Neurosci.* **23**, 4470–4478